Effects of γ-Aminopropyltriethoxylsilane on Morphological Characteristics of Hybrid Nylon-66-Based Membranes Before Electron Beam Irradiation

C.P. Leo,[1] A. Linggawati,[2] A. W. Mohammad,[2] Z. Ghazali[3]

[1]*School of Chemical Engineering, Engineering Campus, Universiti Sains Malaysia, Seri Ampangan,14300 Nibong Tebal, S.P.S., Penang, Malaysia*
[2]*Department of Chemical and Process Engineering, Universiti Kebangsaan Malaysia, 43600 UKM Bangi, Selangor, Malaysia*
[3]*Radiation Processing Division, Malaysian Institute for Nuclear Technology Research (MINT), 43000 Kajang, Selangor, Malaysia*

Received 27 July 2010; accepted 22 February 2011
DOI 10.1002/app.34393
Published online 12 July 2011 in Wiley Online Library (wileyonlinelibrary.com).

ABSTRACT: Nylon-66 is a typical semicrystalline polymer that can be crosslinked using crosslinking agents and electron beam irradiation. Hybrid nylon-66-based membranes are more porous but denser compared to the pure nylon-66 membrane. Besides that, hybrid nylon-66 membranes exhibit higher water uptake and severe swelling in water. Si/nylon-66 membranes were prepared by adding γ-aminopropyltriethoxylsilane (APTEOS). Crosslinked silica in nylon-66 membranes is confirmed with high gel content and Fourier transform infrared peaks, but XRD results showed that there is a low crystalline degree in these membranes. The thermal stability of hybrid nylon-66 membranes is also less affected by APTEOS. The crosslinking agent only improves storage modulus in hybrid nylon-66 membranes. After irradiation, it is learned that APTEOS improves separation performance of nylon-66 membranes. However, excessive APTEOS causes the ratio of effective thickness over porosity ($\Delta x/A_k$) reduces significantly resulting a lower permeability membrane. © 2011 Wiley Periodicals, Inc. J Appl Polym Sci 122: 3339–3350, 2011

Key words: nylon; crosslinking; composites; membranes; electron beam irradiation

INTRODUCTION

Nylon-66 is a polyamide synthesized from 1,6-hexamethylene diamine and adipic acid and contains a mixture of polymer chain with ends terminating in amine, carboxylic acid, or a combination of the two groups. Nylon-66 is commonly used in thermoplastic engineering because of its distinguished characteristics such as excellent thermal stability, great mechanical strength, and high resistance to chemicals.[1] In membrane market, nylon membranes have been commercialized for microfiltration, sterilizing filtration, bioassays, solvent filtration, and particle removal. As nylon-66 is a typical semicrystalline polymer, it can even be crosslinked through electron beam irradiation to form nanofiltration membranes.[2] More importantly, nylon-66 contains functional groups, such as carbonyls, which form hydrogen bond with inorganic silica network and allow the engineering of hybrid membranes.[1]

Correspondence to: A. W. Mohammad (wahabm@vlsi.eng.ukm.my).

Journal of Applied Polymer Science, Vol. 122, 3339–3350 (2011)

Hybrid membranes consisting of organic polymer and inorganic phase are increasingly important due to their remarkable properties such as thermal, mechanical, and separation characteristics compared to pure polymeric membranes.[3] There are various methods of preparing hybrid membranes, producing composites with strong, weak, or without any chemical interactions between components. Sol–gel method offers a simple route in preparing hybrid membranes with hydrogen bonding between polymer and inorganic phases under mild conditions.[4] Inorganic crosslinking agents such as γ-aminopropyltriethoxylsilane (APTEOS), octyltrimethoxylsilane, phenyltrimethoxylsilane, and tretraethoxylsilane (TEOS) are soluble in common organic solvents and allow effective crosslinking reactions.[5] Liu et al.[6] and Peng et al.[7] reported on the preparation of chitosan/silica membranes using γ-glycidoxypropyltrimethoxysilane (GPTMS). Excellent stability of chitosan/silica membranes contributes to great durability in the pervaporation of isopropanol–water[6] and the separation of phenylalanine isomers.[8] Chen et al.[9] later described that APTEOS with a 3-aminopropyl and three ethoxysilane groups works better in the crosslinking of chitosan membrane. Permeation flux and water permselectivity of chitosan/silica

membranes are optimized by adding 10 wt % of APTEOS.[9] Unlike using GPTMS,[10] the swelling degree and water permselectivity of poly(vinyl alcohol) (PVA) membranes in pervaporation can be both improved by using APTEOS.[11] It is reported that hydrophilicity of the hybrid membranes is less affected by amido in APTEOS. The large aminopropyl groups in APTEOS even prevent crystalline region, which increase the permeation flux. Meanwhile, there are works on polyimide/silica membranes prepared using tetramethoxysilane (TMOS), which show higher CO_2/CH_4 selectivity at greater silica content.[12] Jang et al.[13] also reported that APTEOS improves N_2 and O_2 permeability of poly(*N*-vinylpyrrolidone)/APTEOS membranes. Besides that, several research teams recently reported on the preparation of hybrid membranes for fuel cells. It is observed that crosslinked inorganic phase only helps to improve the mechanical integrity of membranes.[14]

As hybrid membranes show enhanced properties in pervaporation, gas separation, and fuel cell, it is interested here to synthesize hybrid nylon-based membranes for nanofiltration. Our previous study[2] reported that electron beam irradiation causes morphological changes on nylon-66 membranes and enhances rejection of neutral and charged solutes. As the rejection of charged solutes by irradiated nylon-66 membranes is less satisfactory, a widely used crosslinking agent, APTEOS, will be added before irradiation to improve morphological properties of nylon membranes for nanofiltration. Effects of crosslinking agents on membrane morphology and functionality differ in various polymeric membranes, such as chitosan-based, PVA-based, and polyamide-based hybrid membranes. Thus, it is definitely important to understand changes in hybrid nylon-based membranes before electron beam irradiation.

EXPERIMENTAL

Membrane preparation

Poly(hexamethylene adipamide) (Nylon-66, Aldrich) was received in pellet form. Formic acid p.a (FA) (Merck, 99%) was used as the solvent. Nylon-66 pellets were initially dried under vacuum at 60°C for 4 h. Dried pellets were thoroughly dissolved in formic acid at 12.5% polymer concentration (w/w) and labeled as N0, representing pure nylon-66 solution. Doped solution for the preparation of hybrid membranes was prepared by adding APTEOS solution at a weight-age ratio of 5 : 95, 10 : 90, and 20 : 80 (APTEOS solution/polymer). The APTEOS solution was prepared by dissolving 1 mol of APTEOS in 4 mol of water. Viscous and homogeneous solutions were left for 24 h to eliminate air bubbles. Casting solution was then uniformly spread on a glass surface using a casting Gardner knife of 1 mm gap, yielding of 350-μm thin films. For morphological, chemical, thermal, and mechanical study before electron beam irradiation, thin films were dried in open air at 25°C for 5 days to form hybrid membranes without electron beam (EB) modification. These membranes were designated as N0, H5, H10, and H20 according to the ratio of added APTEOS solution. On the other hand, some thin films were irradiated before drying step to form hybrid membranes with EB irradiation. These thin films were irradiated using an EB (Alurtron NHV EPS-3000) at 1 MeV accelerating voltage and 10 mA beam current. Irradiation doses used were 70 kGy given during each pass. Thus, these membranes were labeled as N0-70, H5-70, H10-70, and H20-70. EB-irradiated membranes were later tested in filtration experiments. All membrane preparation steps were carried out under room temperature conditions of 25°C with relative humidity of about 60%.

Characterization of physical properties

Membrane morphologies, including top and cross-sectional views, were observed using scanning electron microscopy (SEM, Oxford Instrument 7353, U.K.). For cross-sectional observation, samples were prepared by fracturing membranes in liquid nitrogen and coating with Au by sputtering.

Before the measurement of membrane density and water uptake, membranes were dried at 60°C for 4 h. Density of membranes was determined using Archimedes method. After cooling to room temperature, the density of samples was measured using an electronic densitometer (MD 200S, Japan). For the measurement of water uptake, dried membranes were weighted and immersed in water as stated in ASTM method, D 570-98. Equation (1) was used to calculate the percentage of water uptake.

$$\text{Percentange of water uptake} = \frac{W_w - W_d}{W_d} \times 100\% \quad (1)$$

where W_w is the weight of wet membranes and W_d is the weight of dried membranes.

Contact angle of membranes was measured using face contact anglemeter CA-A. Membranes were vacuum dried for 15 h at 80°C before contact angle measurement. The contact angle of membranes was measured at 15 s after the formation of water droplet at membrane surface.

Membrane swelling in water was measured by immersing dried membranes in for 48 h at room temperature. Water on the surface of the swollen films was removed with cellulose paper, and the film was weighed. Membranes were dried at 60°C

until they reached constant weight. The degree of swelling (%S) is defined in eq. (2):

$$\%S = \frac{1}{\rho_s} \times \frac{W_s - W_d}{W_d} \times 100\% \quad (2)$$

where ρ_s is the solvent density, W_s is the weight of the swollen membrane, and W_d is the weight of dried membrane.

For gel content measurement, membranes were vacuum dried at 80°C for 12 h and portions of the films were weighed. These portions were immersed in 85% formic acid for 3 days at room temperature with small amounts of fresh solvent added every day. Gels were collected by filtering through a fritted glass crucible. The percent gel content was calculated using the following formula.

$$\text{Percentage of gel content} = \frac{W_r}{W_d} \times 100\% \quad (3)$$

where W_r is the weight of residual membranes and W_d is the weight of dried membranes.

Characterization of chemical properties

Fourier transform infrared (FTIR; FTIR Spectrum 2000, Perkin–Elmer, USA) spectra of the membrane films were taken between 500 and 4000 cm^{-1} at room temperature. Besides that, XRD study on membrane films was carried out using Philip Analytical X-ray B.V with a scanning range of 5°–50°, a step size of 0.02°, and a scanning rate of 2 steps/s.

Characterization of thermal properties

Thermal gravimetric analysis (TGA) was performed using TGA Pyris 1 (Perkin–Elmer, USA) over a temperature range of 50–700°C using nitrogen as carrier gas (30 mL/min) and temperature-ramping rate of 10°C/min. Based on TGA results, differential thermal analysis (DTA) was also carried out. Besides that, differential scanning calorimetry was performed using Mettler Toledo 822E in the temperature range of 50–400°C to determine T_m (melting point) of membrane samples.

Characterization of mechanical properties

Dynamic mechanical data (DMA) were obtained using DMA Perkin–Elmer 7e (USA). Membranes were tested in the temperature range of −150 – 300°C with heating rate of 10°C/min and a frequency of 1 Hz.

Filtration experiments

Permeation experiments were conducted with deionized water, vitamin B_{12} solution, and raffinose solution. All solutions were prepared using deionized water. Membranes were immersed in deionized water overnight before being used. All solutions were brought to a constant temperature of 25°C ± 0.2°C in a water bath for at least 1 h before being used. Concentration of vitamin B12 and raffinose was measured using a spectrophotometer (Shimadzu UV-1601PC). Permeation studies were carried out in an Osmonics SEPA ST dead-end cell with a volume of 300 mL and effective membrane area of 15.2 cm^2. The maximum operating pressure of the cell was 450 psig (31 bar). There was a magnetic stirrer assembly inside the cell feed chamber that allowed the use of magnetic stir plates for mixing. The maximum operating stirring speed was 400 rpm with the pressure set between 1 and 28 bar. Permeate was collected in a graduated cylinder.

RESULTS AND DISCUSSION

Effects of APTEOS content on membrane physical properties

All nylon-66-based membranes prepared in this research are thin, brittle, and opaque. Nylon membranes are generally opaque due to the formation of spherulitic structure.[15] During physical inspection, it is observed that increased APTEOS content causes hybrid membranes to be more opague and brittle. This may be due to the poor dispersion of inorganic phase and weak bonding between spherulitic boundaries.[16] Microstructure of membranes is further analyzed using SEM. Figure 1 shows the top and cross section of nylon membranes crosslinked by APTEOS. It is observed that the increased content of APTEOS causes increasing porosity of shperulite surface. More cellular pores are formed in H5, H10, and H20 membranes compared to N0 membrane [Fig. 1(b,d,f,h)]. Nodular spherulite with opening pores (1 μm to few micrometers in diameter) appears on the top surface of hybrid membranes. Macropores are interconnected by micropores as well, but such observation is not reported by others in the utilization of APTEOS for crosslinking chitosan and PVA membranes.[9,17]

Density of nylon-66-based membranes with different loadings of APTEOS is displayed in Figure 2(a). The density of pure nylon-66 membrane is 1.098 g/cm^3, similar to the density of nylon-66 pellets reported by supplier (1.09 g/cm^3). Density of hybrid membranes generally increases with the addition of APTEOS. The observation is similar to the work reported by Zhang et al.,[18] describing that the incorporation of APTEOS in PVA matrix causes an increment of density in hybrid membranes. Hybrid membranes especially H5 and H10 show great increment in density, corresponding to 4.92 and 8.38%.

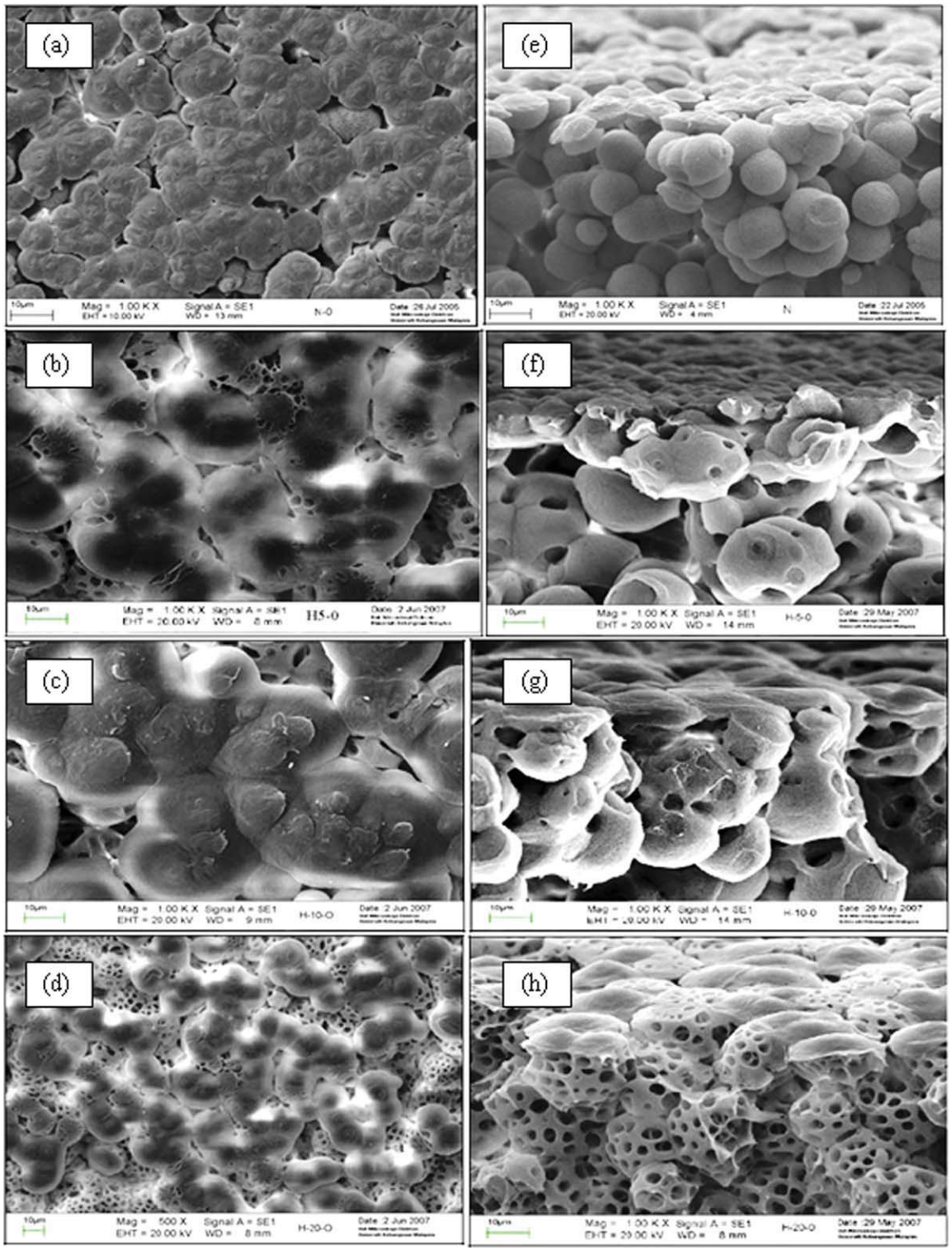

Figure 1 SEM photographs for nylon-66-based membranes: top view of (a) N0, (b) H5, (c) H10, and (d) H20 membranes; cross-sectional view of (e) N0, (f) H5, (g) H10, and (h) H20 membranes. [Color figure can be viewed in the online issue, which is available at wileyonlinelibrary.com.]

Crosslinking can be generally achieved using radiation, peroxide, or silane. In this case, density increment up to 8.38% demonstrates effective silane crosslinking by APTEOS. Crosslinking is resulted from the condensation of SiOH bonding, which forms Si—O—Si by releasing H_2O. Density of H20 membranes only increases 1.55% even though 20 wt % of APTEOS has been used in the membrane

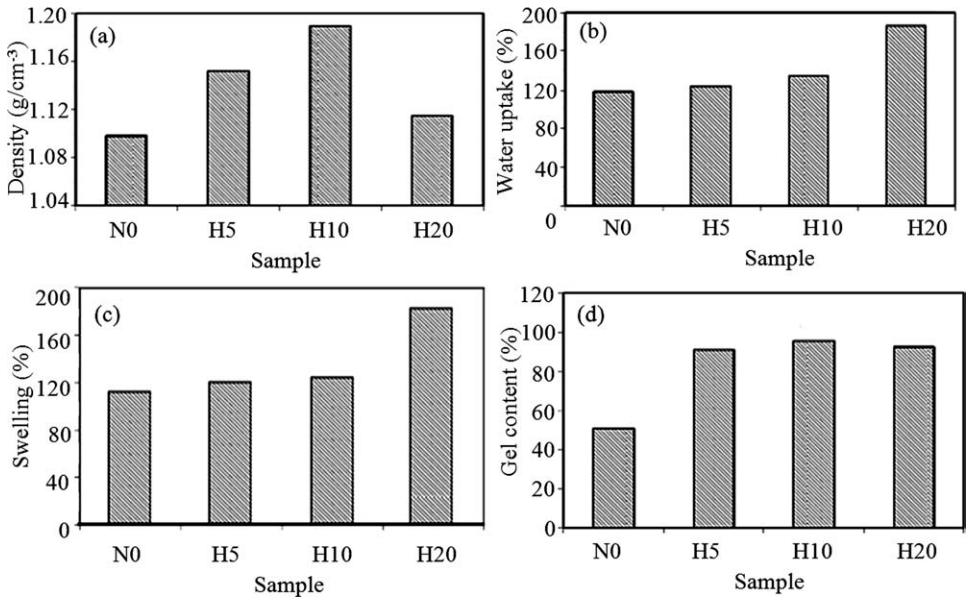

Figure 2 (a) Density, (b) water uptake, (c) swelling, and (d) gel content of nylon-66-based membranes.

preparation. This may due to the formation of extremely porous structure in H20 membranes as illustrated in SEM micrographs.

The percentage of water uptake for nylon-66-based membranes is summarized in Figure 2(b). It is obvious that APTEOS content improve water adsorption of hybrid membranes. The water uptake value of hybrid membranes increases as much as 59.19% compare to pure nylon-66 membranes. The improvement is possibly caused by increasing hydrophilic sites such as amine, silanol, and Si groups resulted from crosslinking. In addition, porosity of hybrid membranes has been greatly enhanced by crosslinking, and it may improve water uptake of hybrid membranes.[19]

Water contact angle of nylon-66-based membranes cannot be measured, because water droplets penetrate into membranes before reaching 15 s. In this study, there is no observation on the increment of membrane hydrophobicity with the addition of APTEOS. The observation is similar to the works reported by Liu et al.[20,21] In their works, it is reported that the hydrophilicity of chitosan/silica membranes is only slightly improved by GPTMS, less than 10° of reduction.

Membrane swelling is commonly influenced by membrane material and solvent. Parameters affecting membrane swelling are membrane hydrophobicity, solvent viscosity, and membrane solubility.[22] In this research, it is learned that APTEOS affects the swelling of nylon-66-based membranes indirectly. Hybrid membranes with morphological changes after crosslinking show higher swelling degree compared to pure nylon-66 membrane [Fig. 2(c)]. The crosslinking agent, APTEOS, is certainly not effective in preventing membrane swelling, because swelling degree of hybrid membranes increases when more APTEOS is added. The growth of swelling degree seems to be contradicting with the common perception that swelling degree reduces when more crosslinking agent is consumed.[9] As discussed in SEM analysis, higher porosity is generated in hybrid membranes, which allow more absorbed water to be accommodated and causes further swelling. Thus, it is reasonable to observe higher swelling degree in hybrid membranes with more crosslinking activities as discussed by Xiao et al.[23]

Gel formation in hybrid membranes confirms the crosslinking reaction between polymeric and inorganic phases. In this work, it is illustrated in Figure 2(d) that the gel content of hybrid nylon-66 membranes relies on APTEOS quantity. Compared to the pure nylon membrane (N0), there is a very huge increment of gel content in H5 and H10 membranes, corresponding to 28.17 and 35.13%. Such results prove that APTEOS successfully initiate crosslinking in nylon-66-based membranes. However, gel content of H20 membranes is slightly lower than gel content of H10 membranes. It may be explained by polymer degradation when excessive crosslinking agent is used.[24] In this research, the observation may also be related to the formation of nonhydrogen bonding in H20 membranes, which is further discussed in FTIR analysis.

Effects of APTEOS content on membrane chemical properties

Hybrid nylon-66-based membranes were prepared using sol–gel method at acidic condition in this

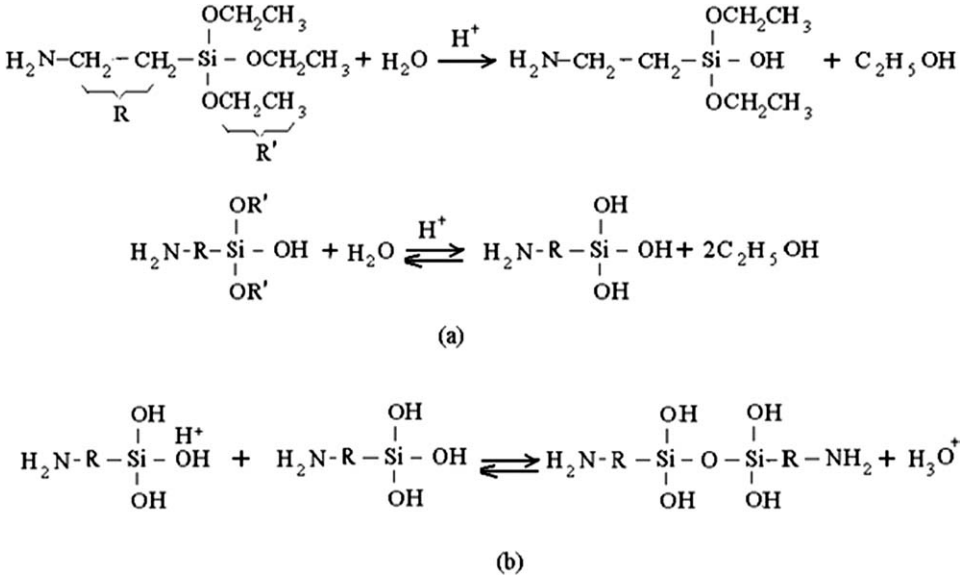

Figure 3 (a) Hydrolysis and (b) condensation reaction of APTEOS.

study. During hydrolysis, silanol will be protonated rapidly at low pH. The protonation of silanol forces silicon to be more electrophilic and susceptible to nucleophilic attack.[25] Hydrolyzed silane crosslinking agent produces Si—OH, which tends to react with other protonated Si—OH groups in the condensation reaction (Fig. 3). Condesation mechanism at acidic condition involves neutral silanol groups and protonated silanol species as shown in Figure 3. Hydrolysis and condensation reactions affect peak intensities and peak pattern of FTIR spectrum for nylon-66-based membranes.

From FTIR spectrum (Fig. 4), all membranes exhibit peak characteristic of nylon-66 such as 3295 cm^{-1}(NH stretching) and 1630 cm^{-1} (C=O stretching and NH stretching vibration in amide I). The band at 1530 cm^{-1} indicates the NH deformation and CN stretching in amide II.[26] Semicrystalline nylon-66 has two more characteristic peaks for the crystalline (935 cm^{-1}) and amorphous (1138 cm^{-1}) as shown in Figures 4 and 5. However, the additional APTEOS in nylon matrix causes an increment in peak intensity. All hybrid membranes exhibit higher peak intensities in the 3294–2850 cm^{-1} region compared to pure nylon-66 membrane. The intense absorption band near 3294 cm^{-1} can be assigned to NH vibrations associated with hydrogen bonding.[27] Higher peak intensity indicates more hydrogen bonding in hybrid membranes. Hydrogen bonding also increases the amide I and amide II band intensities at 1629 and 1534 cm^{-1} (NH plan), respectively, because H bonding occurs with this functional group.[28] As shown in Figure 6, hydrogen bonds

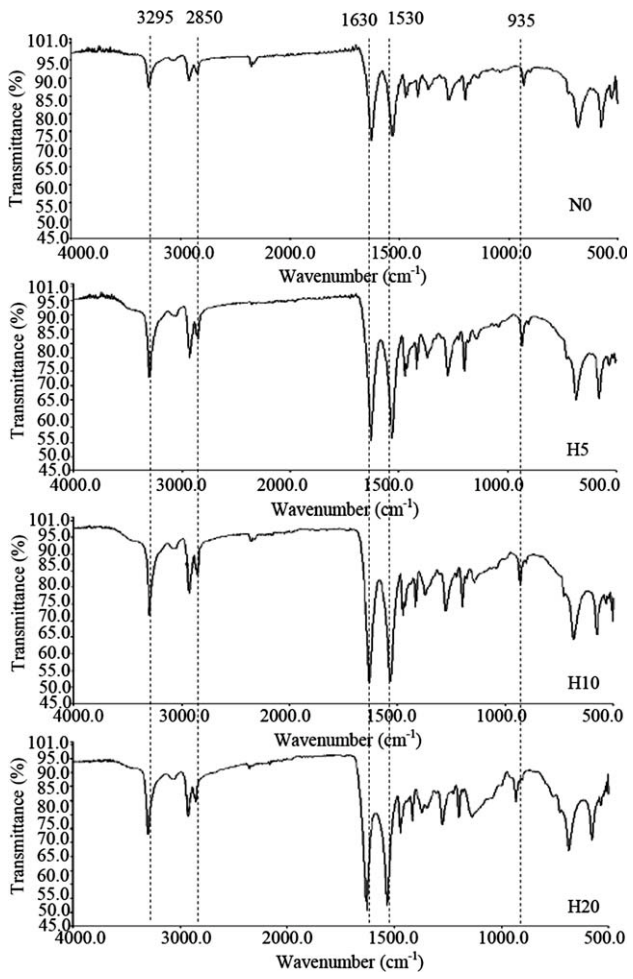

Figure 4 FTIR spectrum for nylon-66 membranes in the range of 4000–500 cm^{-1}.

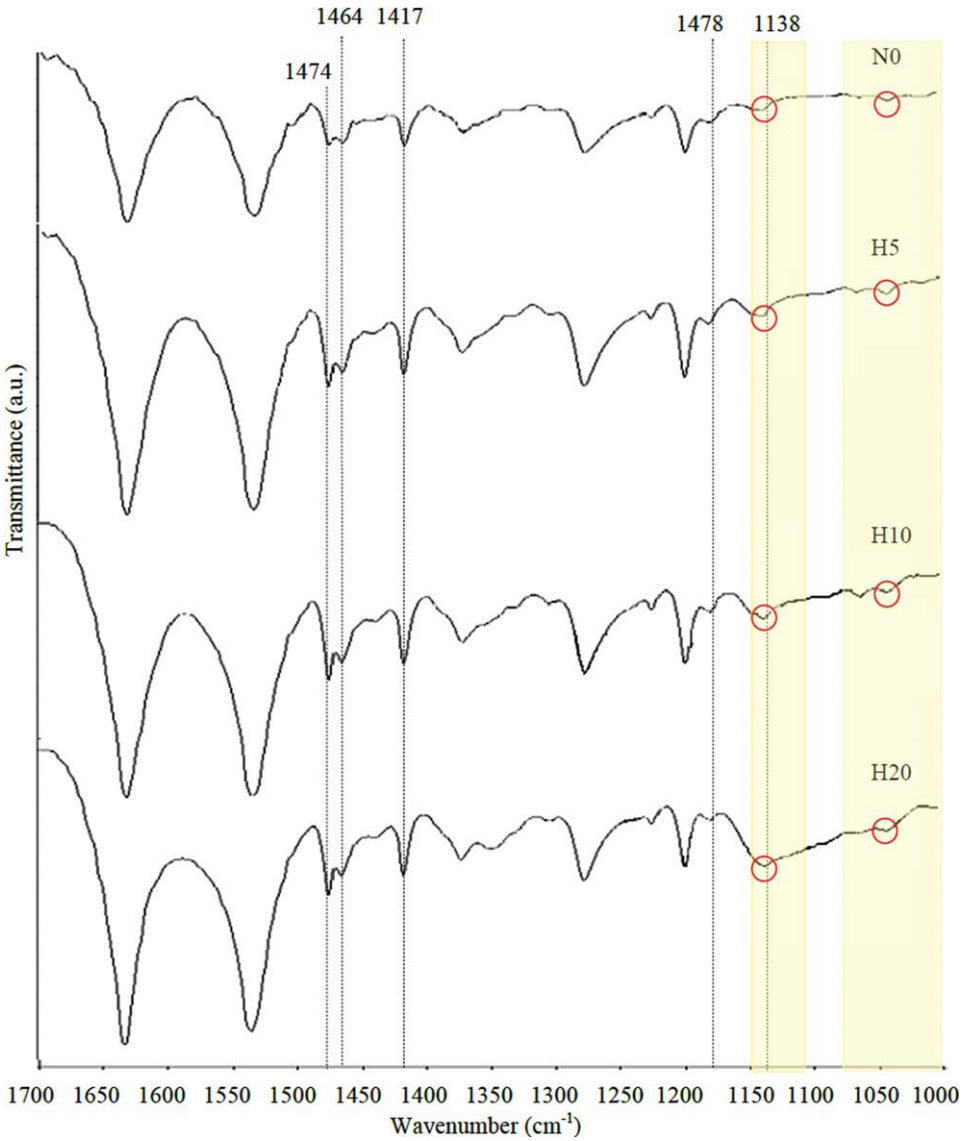

Figure 5 FTIR spectrum for nylon-66 membranes in the range of 1700–1000 cm^{-1}. [Color figure can be viewed in the online issue, which is available at wileyonlinelibrary.com.]

form between NH sites at alkoxy groups and N from amine groups or O from carbonyl groups at amide groups of nylon-66. There is also hydrogen bonding between Si—O and H sites from amine groups. In addition, hydrogen bonds link OH of silanol with N at amine groups or O at carbonyl groups from nylon-66. Incorporating APTEOS in the preparation of hybrid nylon-66 membranes causes some slight changes in the peak position of 3295 and 1530 cm^{-1} for H5, H10, and H20 membranes. The small decrement of peak frequency in H5 and H10, which is related to NH stretching, is possibly due to the growth of hydrogen bonding in these membranes. Meanwhile, the increased peak frequency, which is related to NH deformation, may indicate the formation of nonhydrogen bonding.

Unlike pure nylon-66 membrane, hybrid membranes exhibit double-peak with the high frequency in the 1115–1150 cm^{-1} region and a low frequency in the 1000–1080 cm^{-1} region (Fig. 5). These peaks are the asymmetric stretching frequencies of Si—O—Si units created from the condensation of Si—OH by releasing H_2O.[29] Peaks in the range of 1000–1080cm^{-1} are actually much lower compared to literatures, because the porosity of hybrid membranes is relatively high, which attributed to an incomplete Si—OH condensation.[30] Hybrid membranes also show peaks around 1135 cm^{-1}, which can be related to the amorphous phase of C—C=O.[15] It is observed that H20 membrane has the highest peak intensity at 1135 cm^{-1}, corresponding to the lowest crystalline degree. Besides amorphous phase

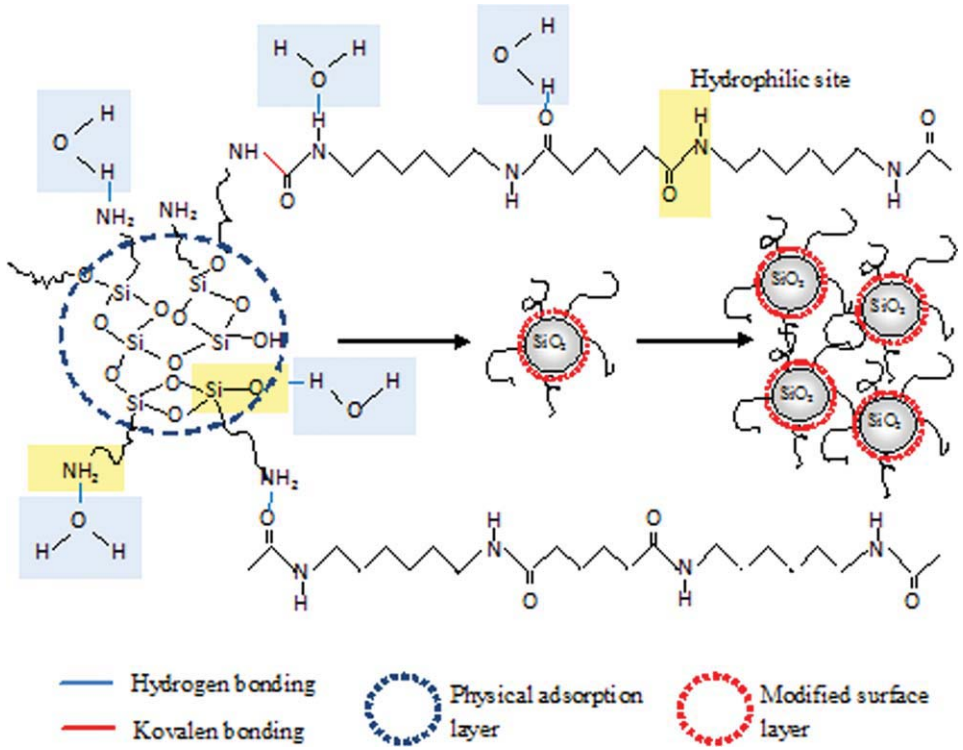

Figure 6 Illustration of the interaction between water molecules and crosslinked nylon-66 membrane. [Color figure can be viewed in the online issue, which is available at wileyonlinelibrary.com.]

of C—C=O, hybrid membranes show weak peaks in the region of 1178 cm^{-1} representing the amorphous phase of NH_2—CH_2.[31] From Figure 5, it is also observed that the incorporation APTEOS in nylon-66 affects peak intensity at 1417, 1464, and 1474 cm^{-1}. These frequencies correspond to scissoring vibration of CH_2 units located near to C=O and CN or CH_2 units located far from amide groups.[32]

Effects of APTEOS on the crystallization of nylon-66 membrane can be studied using XRD spectrum in Figure 7. The 2θ, interplanar spacing (*d*), and peak intensity for all nylon-66-based membranes are tabulated in Table I. Pure nylon-66 membrane (N0) exhibits three diffraction peaks at 20.03°, 24.11°, and 13.33°, corresponding to the reflection of (100), (010, 110), and (002) planes.[33,34] The peaks at 2θ values of 20.03° and 24.11° indicate the formation of α phase in pure nylon-66 membrane. The α_1 peak (2θ = 20.03°) occurs from the distance between hydrogen-bonded chains while the α_2 peak (2θ = 24.11°) arises from the separation of hydrogen-bonded sheets.[35] Besides α phase, nylon-66 membranes also exist in γ phase at room temperature with the occurrence of γ_1 peak at 13.33° and γ_2 peak at 22.2°.[36] In this research, the nylon-66 membranes show γ peak at 13.33° only. This observation is similar to the diffraction pattern of polyamide 6,6/TEOS composites reported by Sengupta et al.[37] The formation of pseudohexagonal structure in nylon-66 membranes is not confirmed, because pseudohexagonal structure contains γ and α phases, which appear at 2θ areas, namely 13.5° (γ_1), 20.2° (α_1), 22.3° (γ_2), and 23.8° (α_2). According to Sengupta et al.,[27] the existence of γ_1 peak may due to artifact added in nylon-66 by the supplier but not due to silica generated in the nylon-66 matrix.

Adding 10 wt % APTEOS in nylon-66 membranes causes an increment of peak intensity as displayed in Figure 7. The increased intensity of α_1 and α_2 diffraction peaks demonstrates a growth in hydrogen-bonded sheets and the separation of hydrogen-bonded sheets. The observation is similar to the

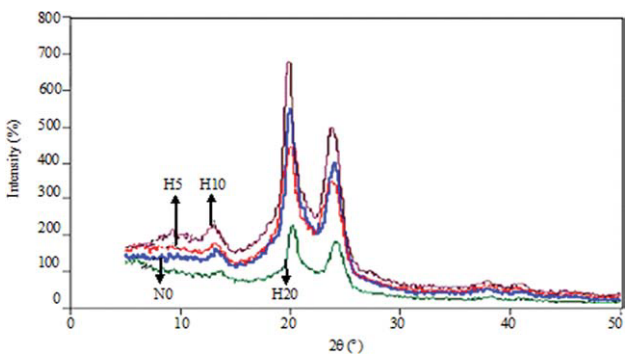

Figure 7 XRD spectrum for nylon-66-based membranes. [Color figure can be viewed in the online issue, which is available at wileyonlinelibrary.com.]

TABLE I
Diffraction Characteristics of Nylon-66 Based Membranes

Sample	2θ (°C)			*d* spacing (nm)			Peak intensity	
	γ	α_1	α_2	γ	α_1	α_2	α_1	α_2
N0	13.33	20.03	24.11	0.66	0.45	0.37	547	397
H5	13.20	20.11	23.81	0.67	0.44	0.37	440	348
H10	13.31	19.91	23.85	0.66	0.45	0.37	675	496
H20	13.64	20.27	24.17	0.65	0.48	0.37	227	182

work reported by Liu et al.,[38] which shows rapid crystallization in PA 6,6 with the addition of nanosilica. However, adding 20 wt % of APTEOS causes much lower α peaks in hybrid membranes compared to pure nylon-66 membrane. A great decrement in crystallinity occurs in H20 membrane is probably due to poor molecular packing.[39] As discussed in SEM analysis and density measurement, a great porosity in H20 membrane causes density of H20 membrane to be the lowest among hybrid membranes. Thus, it is learned in this study that the intensity of α-peaks is not only affected by the growth of hydrogen bonds, but also the molecular packing in hybrid membrane. As the hydrogen bonding is not expected to be greatly formed in H5 membranes, the higher porosity in H5 membranes may cause the slightly lower α-peaks in H5 membranes compared to pure nylon-66 membranes.

Effects of APTEOS content on membrane thermal stability

From the thermal stability study, TGA and DTA results have been summarized in Figures 8 and 9. There are three degradation stages in N-0 and H20 membranes while there are only two degradation stages in H5 and H10 membranes. First degradation stage at temperature less than 100°C is due to the weight loss of surface-adsorped water and water generated from condensation. The temperature of second degradation is measured at 384.91°C, 438.80°C, 440.30°C, and 439.31°C for N0, H5, H10, and H20 membranes. The weight loss happened between 350 and 475°C is resulted from the decomposition of nylon-66 polymer chains into CO_2, H_2O, NH_3, and HCN.[40] For N0 and H20 membranes, the second degradation may be related to the cleavage of relatively unstable part of the polymeric matrix or the structural reorganization of the polysilone. The extra step in weight loss at 454°C and 495.94°C recorded for N0 and H20 membranes may be due to the complete decomposition of the backbone of the polymeric matrix.[41] The absence of the third weight loss region in H5 and H10 membranes is possibly corresponded to the formation of crosslinked matrix.[41] With more APTEOS added into nylon-66 membranes, the total weight loss reduces from N0 membrane to H20 membrane. The observation may be explained by the existence of more silica element in nylon-66 matrix when more APTEOS is used. It is compatible with FTIR analysis where there is an increment of peak intensity at 1134 and 1080 cm^{-1}.

T_d onset and T_d (5 and 10% weight losses) for all nylon-66-based membranes from TGA curves and DTG peak temperature are summarized in Table II. Comparing T_d onset with 5% weight loss in

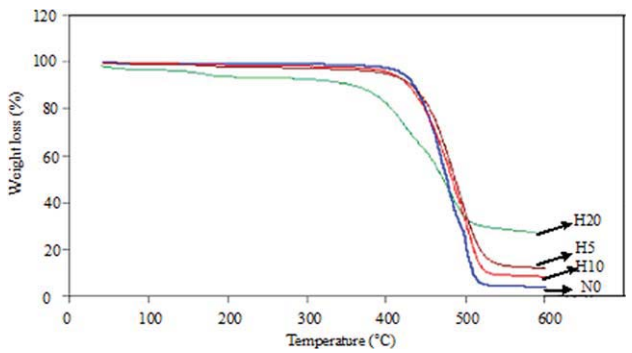

Figure 8 TGA curves for nylon-66-based membranes. [Color figure can be viewed in the online issue, which is available at wileyonlinelibrary.com.]

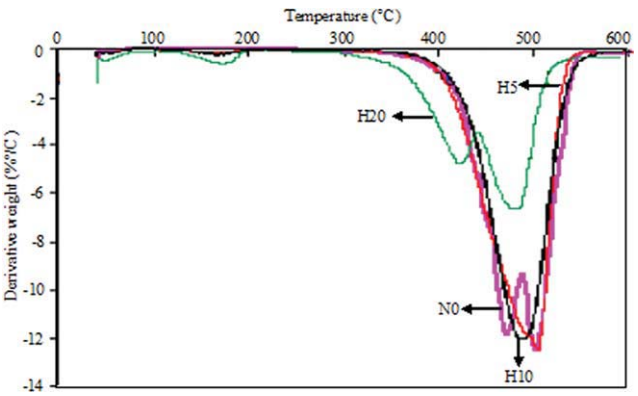

Figure 9 DTA curves for nylon-66-based membranes. [Color figure can be viewed in the online issue, which is available at wileyonlinelibrary.com.]

TABLE II
Thermal Properties of Nylon-66 Based Membranes

Sample	T_d onset (°C)	T_d (°C)	T_m (°C)	Weight residue at 600°C (%)
N0	439.31	504.47	258.32	3.44
H5	438.80	487.24	257.65	7.61
H10	440.30	506.15	258.02	11.42
H20	384.91	481.75	256.55	26.42

membrane samples to evaluate the thermal stability of hybrid membranes, it can be seen that APTEOS does not alter much on the thermal stability of nylon-66-based membranes. Adding 10 wt % of APTEOS only increases another 1°C of T_d onset for H10 membrane. However, a great amount of APTEOS leads to a depression in the thermal stability of H20 membranes. T_d onset of nylon-66 membranes drops 12.4% when 20 wt % of APTEOS is used. Analyzing T_d and T_m for all membranes, it is observed that there are same effects of APTEOS on other thermal characteristics of hybrid nylon-66 membranes. The last of thermal stability at high-APTEOS content may be reasoned on the basis of an inherently weak structure as a result of loss in crystallinity as discussed in XRD.[37] Compared to literatures, APTEOS is most suitable to be used as the crosslinking agent for PVA membranes, because significant improvement of thermal stability has been reported.[18]

Effects of APTEOS content on mechanical properties of membranes

The loss factor or tan (δ) of nylon-66-based membranes in the temperature range of 200–300°C is exhibited in Figure 10. The glass transition temperature (T_g) is determined from the peak of tan (δ) curves. In general, the increased APTEOS content changes patterns of tan (δ) curves. In the lower temperature range (Fig. 10), N0 membrane shows first peak at 50.4°C, which is close to the glass transition temperature of pure nylon membrane as reported by Jin and Huang.[42] H5 membrane shows a slightly lower glass transition temperature of 43.2°C compared to the pure nylon-66 membrane. Adding 5 wt % in nylon-66 membranes obviously induce lower degree of crystallinity as discussed in XRD analysis. The second peak situated between 100 and 150°C in DMA curves, namely, the β_c relaxation is due to the relaxation of the crystalline domain in membranes. A lower intensity value of the tan $(\delta)_2$ peak in H5 and H20 membranes also described poorer crystallinity of H5 and H20 membranes.[43] H10 membrane is the only hybrid membrane showing higher intensity of the tan $(\delta)_2$ peak, which again confirmed a higher crystalline degree in H10 membrane compared to pure nylon-66 membrane. Another interesting observation in this study is the combination of tan $(\delta)_1$ peak and tan $(\delta)_2$ peak for H10 and H20 membranes. The increment of glass transition temperature for H10 and H20 membranes possibly results the movement of tan $(\delta)_1$ peak and the combination of peaks.

The storage modulus of nylon-66 membranes with various APTEOS content is shown in Figure 10. Below 95°C, it is confirmed that the storage modules of nylon-66-based membranes increased with the increase of APTEOS content up to 20 wt % loading. Crosslinked silica element obviously enhances the mechanical properties of nylon-66 membranes. However, the storage modulus of H10 membrane appears to be the highest after 95°C. Crosslinked nylon-66 membranes can be mechanically optimized at higher temperature when appropriate amount of inorganic element is introduced as reported by Yang et al.[43]

Effects of APTEOS content on separation performance of membranes

Pure and hybrid nylon-66 membranes in this study were irradiated for the comparison of separation performance. Table III summarizes the separation results of nylon-66 membranes after irradiation at 70 kG. It is observed that the rejection of vitamin B_{12} is greatly improved when APTEOS is added in nylon-66 membrane. Hybrid nylon-66 membrane with 10 wt % of APTEOS shows the highest rejection of vitamin B_{12} and raffinose after irradiation at 70 kG.

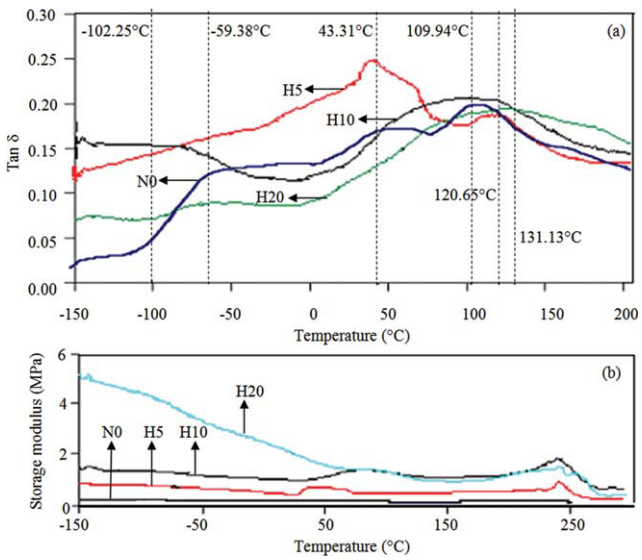

Figure 10 DMA curves for nylon-66-based membranes: (a) Tan δ versus temperature and (b) storage modulus versus temperature. [Color figure can be viewed in the online issue, which is available at wileyonlinelibrary.com.]

TABLE III
Permeability and Salt Rejection of Nylon-66 Based Membranes

Membrane	Water permeability 10^{-11} (ms^{-1} Pa^{-1})	Solute rejection at 15 bar (%)			$\Delta x/A_k$ (μm)
		Vitamine B_{12}	Raffinose	r_p (nm)	
N0–70	3.30	49.06	76.88	1.11	15.34
H5–70	1.14	91.96	78.17	0.96	12.89
H10–70	1.86	92.56	84.97	0.87	12.65
H20–70	1.57	92.60	75.30	1.00	11.16

However, water permeability of nylon-66 membranes is reduced significantly. Fitting Donnan Steric Pore Model into separation results as described previously,[44] it is observed that the increasing APTEOS content reduces membrane pore size (r_p). However, excessive APTEOS content causes the ratio of effective thickness over porosity ($\Delta x/A_k$) reduces significantly in H20-70 membranes. The fitted parameters explain well the separation difference of nylon-66 membranes with different APTEOS contents.

CONCLUSIONS

The addition of APTEOS in nylon-66 membranes affects physical, chemical, thermal, and mechanical properties significantly. Hybrid nylon-66-based membranes are more porous but denser compared to pure nylon-66 membranes. Although hybrid nylon-66 membranes have a higher capability of water uptake, they swell more in water compared to pure nylon-66 membranes. Crosslinked silica in nylon-66 membranes is confirmed with high gel content and FTIR peaks, but XRD results show that there is a low crystalline degree in these membranes. Besides that, the thermal stability of hybrid nylon-66 membranes is less affected by APTEOS. This crosslinking agent only improves storage modulus in hybrid nylon-66 membranes. After irradiation, it is learned that APTEOS improves separation performance of nylon-66 membranes. However, excessive APTEOS causes the ratio of effective thickness over porosity ($\Delta x/A_k$) reduces significantly.

The authors thank Riau Province Government for the scholarship. Also, the authors acknowledge the EB team in the Malaysian Institute for Nuclear Technology Research (MINT) for providing help in using Alurton machine.

References

1. Fried, J. R. In Physical Properties of Polymer Handbook; Mark, J. E., Ed.; Springer Science and Business Media: New York, 2007; Chapter 13.
2. Linggawati, A.; Mohammad, A. W.; Ghazali, Z. Eur Polym J 2009, 45, 2797.
3. Guizard, C.; Bac, A.; Barboiu, M.; Hovnanian, N. Sep Purif Technol 2001, 25, 167.
4. Livage, J. Bull Mater Sci 1999, 22, 201.
5. Zhan, X.; Li, J.; Huang, J.; Chen, C. Chin J Polym Sci 2009, 27, 533.
6. Liu, Y. L.; Su, Y. H.; Lee, K. R.; Lai, J. Y. J Membr Sci 2005, 251, 233.
7. Peng, F. B.; Lu, L. Y.; Sun, H. L.; Wang, Y. Q.; Liu, J. Q.; Jiang, Z. Y. Chem Mater 2005, 17, 6790.
8. Jiang, Z.; Yu, Y.; Wu, H. J Membr Sci 2006, 280, 876.
9. Chen, J. H.; Liu, Q. L.; Zhang, X. H.; Zhang, Q. G. J Membr Sci 2007, 292, 125.
10. Guo, R.; Hu, C.; Pan, F.; Wu, H.; Jiang, Z. J Membr Sci 2006, 281, 454.
11. Zhang, Q. G.; Liu, Q. L.; Jiang, Z. Y.; Chen, Y. J Membr Sci 2007, 287, 237.
12. Suzuki, T.; Yamada, Y. Polym Bull 2005, 53, 139.
13. Jang, K.; Kim, J. S.; Lee, S.; Kim, H. Diffus De B 2007, 124, 683.
14. Chen, J.; Asano, M.; Maekawa, Y.; Yoshida, M. J Polym Sci Part A: Polym Chem 2008, 46, 5559.
15. Kohan, M. I. Nylon Plastics; Wiley: New York, 1973.
16. Lim, S. J.; Noda, I.; Im, S. S. Polymer 2007, 48, 2745.
17. Zhang, Q. G.; Liu, Q. L.; Chen, Y.; Chen, J. H. Ind Eng Chem Res 2007, 46, 913.
18. Zhang, Q. G.; Liu, Q. L.; Jiang, Z. Y.; Ye, L. Y.; Zhang, X. H. Microporous Mesoporous Mater 2008, 110, 379.
19. Cornelius, C.; Hibshman, C.; Marand, E. Sep Purif Technol 2001, 25, 181.
20. Liu, Y. L.; Su, Y. H.; Lai, J. Y. Polymer 2004, 45, 6831.
21. Liu, Y. L.; Hsu, C. Y.; Su, Y. H.; Lai, J. Y. Biomacromolecules 2005, 6, 369.
22. Doig, S. D.; Boam, A. T.; Livingston, A. G.; Stuckey, D. C. J Membr Sci 1999, 154, 127.
23. Xiao, S.; Feng, X.; Huang, R. Y. M. J Membr Sci 2007, 306, 36.
24. Greco, A.; Maffezzoli, A.; Jiménez, A.; Tendero, P. M. R. In Polymer Analysis, Degradation, and Stabilization; Zaikov, G. E., Jiménez, A., Ed.; Nova Science Publisher: New York, 2005.
25. Brinker, C. J.; Scheher, G. W. Sol-Gel Science. The Physics and Chemistry of Sol Gel Processing; Academic Press: San Diego, 1990.
26. Kojima, Y.; Matsuoka, T.; Takahashi, H. J Appl Polym Sci 1999, 74, 3254.
27. Seisler, H. W.; Holland, K.; Moritz, T. Infra Red and Raman Spectroscopy of Polymers; Marcell Dekker: New York, 1980.
28. Kuo, P. C.; Sahu, D.; Yu, H. H. Polym Deg Stab 2006, 91, 3097.
29. Chen, H. J.; Fu, M. Macromolecules 2007, 40, 2079.
30. Ciaramella, F.; Jousseaume, V.; Maitrejean, S.; Verdier, M.; Remiat, B.; Zenasni, A.; Passemard, G. Thin Solid Films 2006, 495, 124.
31. Gonçalves, E. S.; Poulsen, L.; Ogilby, P. R. Polym Deg Stab 2007, 92, 1977.
32. Pages, P.; Carrasco, F.; Saurina, J.; Colom, X. J Appl Polym Sci 1996, 60, 153.
33. Starkweather, H. W.; Jones, G. A. J Polym Sci Polym Phys Ed 1981, 19, 467.

34. Nehme, O. A.; Gabriel, C. A.; Farries, R. J.; Thomas, E. L.; Malone, M. F. J Appl Polym Sci 1988, 35, 1955.
35. Murthy, N. S.; Curran, S. A.; Aharoni, S. M.; Minor, H. Macromolecules 1991, 24, 3215.
36. Bunn, C. W.; Garner, E. V. Proc R Soc 1947, 189 A, 39.
37. Sengupta, R.; Sabharwal, S.; Tikku, V. K.; Somani, A. K.; Chaki, T. K.; Bhowmick, A. K. Polymer 2005, 46, 3343.
38. Liu, X.; Wu, Q.; Berglund, L. A.; Qi, Z. Macromol Mater Eng 2002, 287, 515.
39. Cho, J. W.; Sul, K. I. Polymer 2001, 42, 727.
40. Herrera, M.; Matuschek, G.; Kettrup, A. Chemospher 2001, 42, 601.
41. Xi, F.; Wu, J.; Lin, X. J Chromatorgr A 2006, 1125, 38.
42. Jin, Y.; Huang, R. Y. J Appl Polym Sci 2003, 36, 1799.
43. Yang, C. C.; Chiu, S. J.; Chien, W. C.; Chiu, S. S. J Power Sources 2010, 195, 2212.
44. Bowen, W. R.; Mohammad, A. W.; Hilal, N. J Membr Sci 1997, 126, 91.